Chemical Science

EDGE ARTICLE

View Article Online
View Journal | View Issue

Cite this: *Chem. Sci.*, 2019, **10**, 4192

All publication charges for this article have been paid for by the Royal Society of Chemistry

Received 12th January 2019
Accepted 5th March 2019

DOI: 10.1039/c9sc00190e

rsc.li/chemical-science

Construction of a cross-layer linked G-octamer *via* conformational control: a stable G-quadruplex in H-bond competitive solvents†

Ying He,‡[a] Yanbin Zhang,‡[b] Lukasz Wojtas,[a] Novruz G. Akhmedov,[c] David Thai,[a] Heng Wang,[a] Xiaopeng Li,[a] Hao Guo *[b] and Xiaodong Shi *[a]

Methanol soluble and stable guanosine octamers were successfully achieved *via* H-bond self-assembly. Through structural conformational design, we developed a new class of guanosine derivatives with modification on guanine (8-aryl) and ribose (2′,3′-isopropylidene). This unique design led to the formation of the first discrete G_8-octamer with its structure characterized by single crystal X-ray diffraction, MS and NMR spectroscopy. The G_8-octamer showed unique cation recognition properties, including the formation of a stable Rb^+ templated G-quadruplex. Based on this observation, further modification on the 8-aryl moiety was performed to incorporate a cross-layer H-bond or covalent linkage. Similar G-octamers were obtained in both cases with structures confirmed by single crystal X-ray diffraction. Furthermore, the covalently linked G-quadruplex exhibited excellent stability even in MeOH and DMSO, suggesting a promising future for this new H-bond self-assembly system in biological and material applications.

Introduction

Non-covalent interactions enable construction of large structural motifs from small molecules.[1–3] Molecular self-assembly, an important process typically driven by non-covalent interactions, is often dynamic and generally under thermodynamic control.[4,5] With interest in the application of the self-assembly process to biomedical research, there is a growing demand with respect to preparing stable non-covalent assemblies in a biocompatible environment.[6–8] However, supramolecular structures built through H-bonds are often studied in less polar aprotic solvents (such as CH_2Cl_2) to avoid the competition of H-bond interactions between substrates and solvents.[9,10] Thus, the development of novel supramolecular systems which are stable in a polar protic solvent is highly desirable, though very challenging.[11,12]

A G-quartet is an interesting supramolecular scaffold formed by H-bonds.[13,14] As shown in Scheme 1, with an approximately 90-degree angle between the H-bond donor and acceptor, four guanine units are held together to form a G-quartet. Through ion–dipole interactions, alkali and alkaline earth metal cations can enhance the process by serving as the template to coordinate with central oxygen atoms.[15–17] Stacking of G-quartets gives G-quadruplexes as bioactive building blocks found in DNA and RNA folding.[18,19] In this case, the extent of G-quartet stacking in a G-quadruplex will be determined by the phosphate backbone, which is often associated with the formation of a counter folding subunit, such as the i-motif.[20]

Inspired by this unique H-bond assembly, researchers have been devoted to developing guanine derivatives to achieve controllable G-quadruplex formation from small molecules.[21–23] Some interesting applications have been identified with various G-quartet assemblies, including lipophilic ion channels,[24–26] supramolecular hydrogels,[27–29] nanomaterials,[30,31] potential targets for cancer therapy,[32,33] and more.[34–37] Although many examples of G-quartet formation through various modified

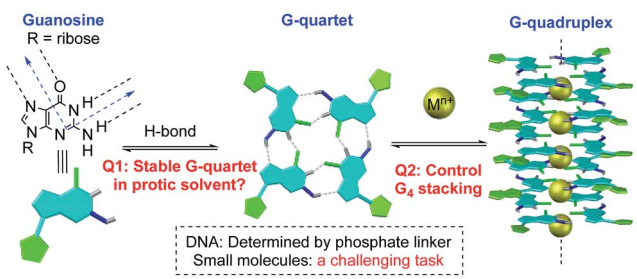

Scheme 1 G-quadruplex formation: equilibrium and stability.

[a]Department of Chemistry, University of South Florida, 4202 E. Fowler Avenue, Tampa, Florida 33620, USA. E-mail: xmshi@usf.edu

[b]Department of Chemistry, Fudan University, 2005 Songhu Road, Shanghai, 200438, People's Republic of China

[c]Department of Chemistry, West Virginia University, Morgantown, WV 26505, USA

† Electronic supplementary information (ESI) available: Experimental section, NMR spectra, ESI-MS spectra and crystallographic data. CCDC 1871565–1871570 and 1871754. For ESI and crystallographic data in CIF or other electronic format see DOI: 10.1039/c9sc00190e

‡ Equal contribution.

guanine derivatives have been reported, studies on controlling G-quartet stacking molecularity are relatively rare.[38,39] Factors to be taken into consideration include the cation concentration,[39] the solvent,[40] the anion,[41] and so on.[42] In many cases, mixtures of various "stacking isomers" (G_8, G_{12} or G_{16}) were observed, which highlights the significant challenges associated with controlling the vertical stacking.[43–46] Moreover, the assembly of a specific and stable G-quadruplex in H-bond competitive solvents remains a challenging task.[48] Herein, we report the construction of the first G-octamer with structures characterized by single crystal X-ray diffraction through monomer conformational design. Moreover, with this new system, stable G-quadruplexes were formed with significantly improved stability. Through the design of cross-layer H-bonds and covalent linkage, G-octamers were prepared with excellent stability in MeOH (no dissociation) and even in 50% DMSO, which offers a potential opportunity to extend the H-bond assembly system into biosystems for future applications.

Results and discussion

Design, synthesis and characterization of G-octamers

Ideally, a G_4-tetramer would be the most concise target towards the construction of a simple and stable assembled structure. However, with a metal template in solution, further stacking of G_4-tetramers leads to the mixture of G-quadruplex species.[49] Thus, G_4-tetramers are unfavorable for the formation of well-defined supermolecules.

The simplest plausible G-quadruplex would be a G-octamer which is likely to adopt either top-to-top (T–T) or bottom-to-bottom (B–B) stacking patterns (Scheme 2A).[50] In previous studies, Meijer *et al.* employed different concentrations of a guanosine derivative resulting in the formation of tunable G-octamers.[41] Spada has reported G-octamer formation upon exposure to UV light through alkene isomerization.[51] Wu presented several excellent examples of G-octamer formation through π–π interactions using NMR and MS studies.[52] Hirao and coworkers applied Au(I)–Au(I) interaction between two G-quartet layers to achieve a G-octamer confirmed by NMR and CD spectra.[53] However, to the best of our knowledge, no single crystal structure of a G-octamer has ever been reported, implying the challenging nature of preparing a stable and discrete G-octamer in a dynamic equilibrium.

To tackle this problem, we set out to design a G-derivative where the structure is rigid and predisposed for the conformation of a potential octamer structure so as to minimize the entropy cost involved in the self-assembly process. As shown in Scheme 2B, modification of guanosine often occurs on two positions: C-8 of purine and the hydroxyl of ribose. The Sessler group first reported on 8-aryl substituted guanosine in the formation of a G-quartet without templating cation in both solution and solid state.[54]

This seminal work initiated the concept of conformational control for G-quartet formation: the steric effect between the aryl substituent and protected ribose helped guanosine to adopt a *syn* conformation, preventing the ribbon formation and giving a tetramer as the dominant conformation. On the other hand, Davis's group developed lipophilic guanosine with bulky ribose to form a G-hexadecamer (Scheme 2B) both in solution and solid state (M^{n+} = K^+, Ba^{2+}, Sr^{2+}, and Pb^{2+}).[55] Notably, a picrate anion bridge played a crucial role: as revealed by single crystal X-ray diffraction (Scheme 2C), four picrate anions linked two G-octamers through H-bonds between anion and two inner G-quartets. The two G-octamers (from adjacent inner and outer G_4) gave top-to-bottom stacking with ribose interdigitated between the adjacent layers. Interestingly, the two inner layers adopted bottom-to-bottom (B–B) stacking, which is more favorable than the T–T mode with the cation binding on the more "naked" convex face between the two layers. This result aroused our interest in developing a G-octamer through similar B–B stacking.

Considering the steric interaction between the C-8 substituent and ribose, we postulated that incorporation of C-8 aryl and the rigid ribose ring might provide a new system with steric hindrance between the G-quartet to force the G_4 bowls to stack in a bottom-to-bottom manner, while obstructing ribose interdigitation at the top-face (Scheme 2C). To confirm this idea, compound **1b** was designed, prepared and applied to assemble with various alkali and alkaline earth metal cations. ^{1}H NMR spectra were obtained and selected regions of the ^{1}H NMR spectra of these G-quadruplexes were compared with the G-hexadecamer from **1a** as shown in Fig. 1.

As previously reported, treating **1a** with alkali and alkaline earth metal salts (K^+, Ba^{2+}, Sr^{2+} and so on) gave two sets of signals in the ^{1}H NMR spectra, corresponding to the inner and outer G-quartet.[56] Conducting similar cation binding experiments with **1b** in $CDCl_3$ gave a single set of ^{1}H NMR signals in all cases (M = K^+, Ba^{2+}, and Sr^{2+}; A^- = Picrate$^-$ or PF_6^-). Furthermore, ESI-MS demonstrated a clear doubly charged

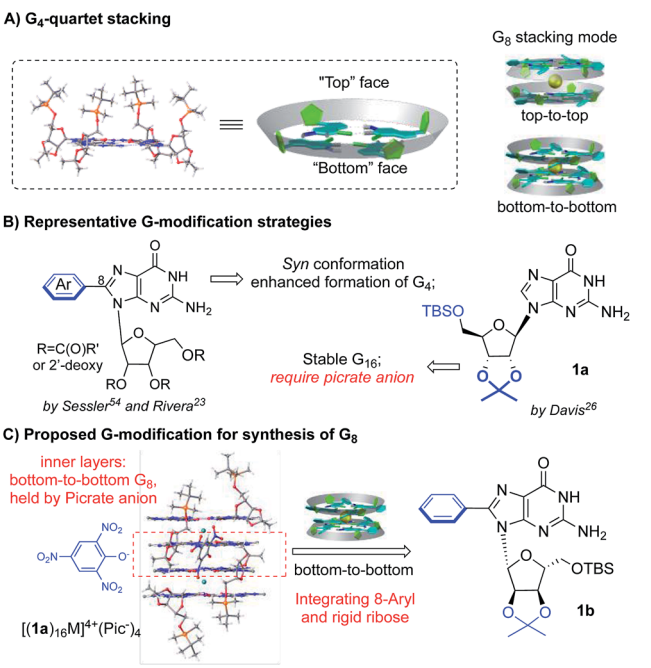

Scheme 2 Achieving a stable G-octamer by controlling G-quartet stacking.

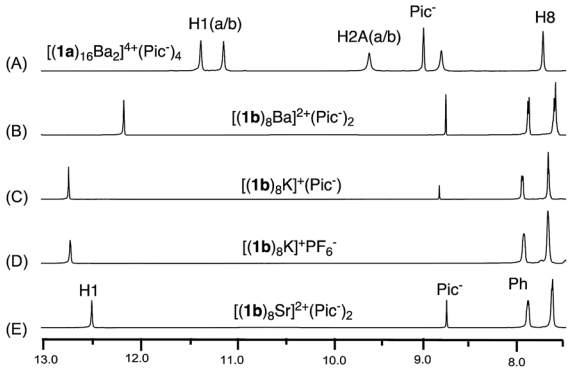

Fig. 1 ^{1}H NMR spectra of G-quadruplexes (A) $[(\mathbf{1a})_{16}Ba_2]^{4+}\cdot(Pic^-)_4$; (B) $[(\mathbf{1b})_8Ba]^{2+}\cdot(Pic^-)_2$; (C) $[(\mathbf{1b})_8K]^+\cdot(Pic^-)$; (D) $[(\mathbf{1b})_8K]^+\cdot(PF_6^-)$; (E) $[(\mathbf{1b})_8Sr]^{2+}\cdot(Pic^-)_2$ in $CDCl_3$.

peak at $m/z = 2123.01$, corresponding to a mol. wt of 4246.68 for $[(\mathbf{1b})_8Ba]^{2+}$. The experimental and calculated isotope patterns further suggested an octameric composition. In addition, traveling wave ion mobility-mass spectrometry (TWIM-MS)[57] confirmed no formation of stacking isomers, which excluded the formation of random aggregates in gas phase (see ESI† for details).

Finally, single crystal structures were obtained and unambiguously verified the G_8-octamer formation with the proposed bottom-to-bottom stacking (Fig. 2A). The top view of the crystal structure (Fig. 2B) shows the G-quartet self-assembly in the tail to tail orientation. The five crystal structures obtained with ligand **1b** include monovalent cations (K^+ and Rb^+) and divalent cations (Ba^{2+} and Sr^{2+}). Picrate anion showed no clear binding with the G-quartet, consistent with what was observed in the ^{1}H NMR spectra (see Fig. S2†). A complex with non-coordinated PF_6^- anion was also successfully obtained, $[(\mathbf{1b})_8K]^+\cdot(PF_6^-)$, confirming the "anion-free" binding mode of this new type of G_8-quadruplex. The distances of the H-bond within the G_4-quartet and between the G_4 layers are compared in Table 1.

According to these crystal structures, all G-octamers from **1b** gave G-quartets with an (N1···O6) and (N2···N7) H-bond distance of around 2.9 Å, similar to that of the inner and outer layer in the G_{16}-hexadecamer formed from **1a**.[46] These results indicated that both cations and the C-8 phenyl substituent had little influence on the H-bond in the G_4-quartet.

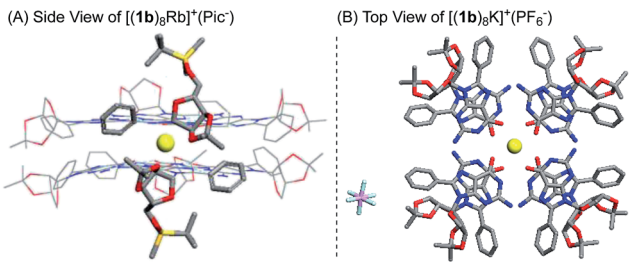

Fig. 2 X-ray single crystal structure of the G_8-octamer (A) $[(\mathbf{1b})_8Rb]^+\cdot(Pic^-)$; (B) $[(\mathbf{1b})_8K]^+\cdot(PF_6^-)$. Similar structures for $[(\mathbf{1b})_8K]^+\cdot(Pic^-)$, $[(\mathbf{1b})_8Ba]^{2+}\cdot(Pic^-)_2$ and $[(\mathbf{1b})_8Sr]^{2+}\cdot(Pic^-)_2$ were also obtained.§

However, the size of the G_8 was influenced by the average O–M distances of all these complexes from **1b**, which might follow the trend where higher ionic potential (Z/r) resulted in shorter O–M distance (2.75–2.81 Å). Interestingly, in comparison with the G_{16}-hexadecamer $[(\mathbf{1a})_{16}Ba_2]^{4+}\cdot(Pic^-)_4$, the G_8-octamers $[(\mathbf{1b})_8Ba_2]^{2+}\cdot(Pic^-)_2$ gave a slightly shorter distance between the two G_4 layers (2.89 Å *vs.* 3.06 Å and 3.58 Å). This result implied the stronger cation interaction of the $(\mathbf{1b})_4$-quartet than the $(\mathbf{1a})_4$-quartet. This improved cation interaction has been supported by G_4-binding studies with Rb^+ using the **1b** ligand and led to the first crystal structures of Rb^+ coordinated G-quadruplexes. Among all the G_8 crystals, $[(\mathbf{1b})_8Rb]^+\cdot(Pic^-)$ gave the longest O–M and G_4–G_4 distance due to its large radii[58] and low valency. Very few examples of Rb coordinated G-quartets have been reported so far, indicating how challenging it is for guanosine to bind with Rb to form a discrete G-quadruplex.[59] To the best of our knowledge, this is the first single crystal structure of a G-quadruplex containing Rb^+, clearly suggesting the promising cation binding ability of guanosine derivative **1b**.

Having successfully confirmed a new concise G_8-quadruplex structure in solution (NMR), solid state (XRD) and gas phase (ESI-MS and TWIM-MS), we evaluated its stability in MeOH. Dissolving octamer $[(\mathbf{1b})_8K]^+\cdot(Pic^-)$ in CD_3OD gave a mixture of two sets of signals in NMR spectra, suggesting partial decomposition of this G_8-octamer (*vide infra*). To obtain MeOH stable G-quadruplexes, further modification is still needed.

Cross-layer H-bonded G-octamers

To further improve the stability of the G-quadruplex, we sought to establish the interactions between the G-quartet layers. As highlighted in Fig. 2A, the 8-phenyl group in **1b** adopted a tilted conformation and reached out from the G-quartet. This geometry provided an opportunity to further enhance the supramolecular structure by introducing new interactions between the two G-quartets.

Notably, the Rivera group have reported the formation of an intralayer H-bond between carbonyl oxygen with N(2)H within the same G-quartet by using 2′-deoxy guanosine derivatives without rigid ribose functionalization.[34,36–38] This work suggested the possibility of forming extra H-bonds by using both hydrogens of the N(2)–NH_2 group. Inspired by this work, a carbonyl group was introduced at the *meta*-position of the 8-aryl position of **1b** as illustrated in Fig. 3A. Based on this design, we hypothesized that N(2)–H_A would form a H-bond with neighboring guanosine within the G-quartet, while the N(2)–H_B could interact with the carbonyl group by forming a cross-layer H-bond.

To confirm this idea, compound **1c** was synthesized and applied to G-quadruplex construction upon interacting with metal cations. According to the ^{1}H NMR spectra, treating **1c** with $Ba(Pic)_2$ led to the formation of a new G-quadruplex with one set of signals, similar to the G_8-octamer obtained from **1b**. Analysis of the NMR sample (in $CDCl_3$) by ESI-MS gave a dominant, doubly charged peak with m/z at 2291.34, corresponding to $[(\mathbf{1c})_8Ba]^{2+}$ (mw = 4582.68).

Table 1 G-quadruplex structural comparison (Å)

G-quadruplex		d(N1···O6)	d(N2···N7)	d(O–M)	d(G_4–G_4)
$[(\mathbf{1a})_{16}Ba_2]^{4+}\cdot(Pic^-)_4$[a]	Inner	2.92 ± 0.01	2.91 ± 0.07	2.75 ± 0.02	3.06 (i–o)
	Outer	2.86 ± 0.01	2.89 ± 0.04	2.79 ± 0.03	3.58 (i–i)
$[(\mathbf{1b})_8K]^+\cdot(Pic^-)$		2.82 ± 0.08	2.87 ± 0.04	2.72 ± 0.17	2.85
$[(\mathbf{1b})_8K]^+\cdot(PF_6^-)$		2.82 ± 0.04	2.89 ± 0.05	2.77 ± 0.03	2.96
$[(\mathbf{1b})_8Ba]^{2+}\cdot(Pic^-)_2$		2.89 ± 0.04	2.89 ± 0.04	2.72 ± 0.05	2.89
$[(\mathbf{1b})_8Sr]^{2+}\cdot(Pic^-)_2$		2.83 ± 0.03	2.86 ± 0.04	2.62 ± 0.05	2.75
$[(\mathbf{1b})_8Rb]^+\cdot(Pic^-)$		2.85 ± 0.03	2.89 ± 0.03	2.81 ± 0.05	3.04

[a] See ref. 46.

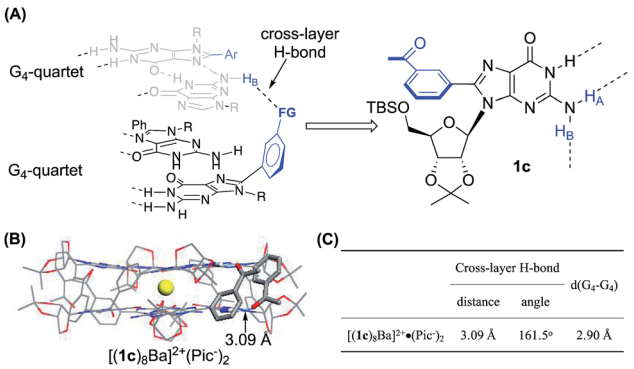

Fig. 3 (A) General design of establishing a cross-layer H-bond; (B) single crystal structure and (C) H-bond information of $[(\mathbf{1c})_8Ba]^{2+}\cdot(Pic^-)_2$.§

Having confirmed the G_8-octamer $[(\mathbf{1b})_8Ba]^{2+}\cdot(Pic^-)_2$ formation, our next goal was to determine if there was a cross-layer H-bond as designed above. The ^1H NMR spectra of $[(\mathbf{1b})_8Ba]^{2+}\cdot(Pic^-)_2$ and $[(\mathbf{1c})_8Ba]^{2+}\cdot(Pic^-)_2$ did not show peaks corresponding to N(2)H at room temperature. This is likely due to the rapid exchange between the two NH_2 protons, even with the formation of a H-bond. Thus, the exchange rate of the two protons provides a direct indication of the H-bond strength in the G_4-quartet. To explore the dynamic structure, variable temperature (VT) NMR experiments with $[(\mathbf{1b})_8Ba]^{2+}\cdot(Pic^-)_2$ and $[(\mathbf{1c})_8Ba]^{2+}\cdot(Pic^-)_2$ were performed and are summarized in Fig. 4.

For complex $[(\mathbf{1c})_8Ba]^{2+}\cdot(Pic^-)_2$, the NH_2 protons started appearing as broad peaks at 0 °C with the chemical shift at 10.28 ppm (H_A) and 7.25 ppm (H_B). In contrast, the VT NMR spectra of $[(\mathbf{1b})_8Ba]^{2+}\cdot(Pic^-)_2$ did not show apparent peaks of the N(2)–H signals until further cooling the sample to −40 °C. The results indicated that there might be an extra H-bond in the **1c** complex to lock the N(2)–NH_2 from rapid exchange. Furthermore, a significantly downfield shifted chemical shift (7.25 ppm) was ascribed to the N(2)–H_B proton in the $(\mathbf{1c})_8$-octamer compared with the $(\mathbf{1b})_8$-octamer (5.98 ppm). These observations provide clear evidence of the formation of a cross-layer H-bond in the $(\mathbf{1c})_8$-octamer as designed.

Finally, the G_8-octamer was verified by X-ray crystallography as shown in Fig. 3B. The crystal structure also confirmed the presence of the cross-layer interactions with a mean H-bond distance of 3.09 Å and a bond angle of 161.5°, suggesting a weak cross-layer H-bond present in solid state (Fig. 3C). This makes the structure a "self-assembled molecular-cuboid" purely constructed by H-bond linkage with all eight guanosine units. On the other hand, the distance of the two G-quartet layers (2.90 Å) in $[(\mathbf{1c})_8Ba]^{2+}\cdot(Pic^-)_2$ remained similar to the **1b** complex. Considering the specific "cage" size in the G_8-octamer shown in Table 1, the cross-layer H-bond was not strong enough to generate extra enthalpy gain to balance the entropy cost caused by holding the two layers tighter.

With the confirmed cross-layer H-bonds, we evaluated the complex stability of $[(\mathbf{1c})_8K]^+\cdot(Pic^-)$ in methanol. The results showed a similar stability to the complex formed with **1b** (*vide infra*). Although the cross-layer H-bond approach could not boost G_8-quadruplex stability in MeOH as anticipated, it provided an effective and novel approach to enhance G-quadruplex stability from monomer conformational design. Structural amendment was required to further improve the stability of the G_8-octamer.

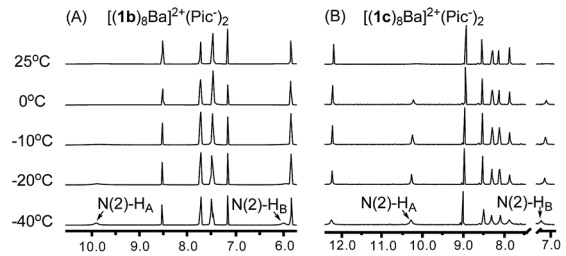

Fig. 4 (A) VT NMR spectra of $[(\mathbf{1b})_8Ba]^{2+}\cdot(Pic^-)_2$ and (B) VT NMR spectra of $[(\mathbf{1c})_8Ba]^{2+}\cdot(Pic^-)_2$ confirmed the cross-layer H-bond design in establishing a cross-layer H-bond.

Cross-layer linkage through a covalent bond

To increase the stability to a new level, we turned to establishing a potential covalent linkage between the two G-quartets. By scrutinizing the crystal structure of $[(\mathbf{1b})_8Ba]^{2+}\cdot(Pic^-)_2$, we found that the distance between the two *meta* position of the phenyl ring from each tetramer was 4.0 Å, a distance similar to three single bond lengths.[58] According to the observation, the *meta* position of the two phenyl groups could serve as a reference site for constructing cross-layer covalent linkers. The guanosine dimer **1d** and **1d′** were then prepared using the synthetic route summarized in Fig. 5A.

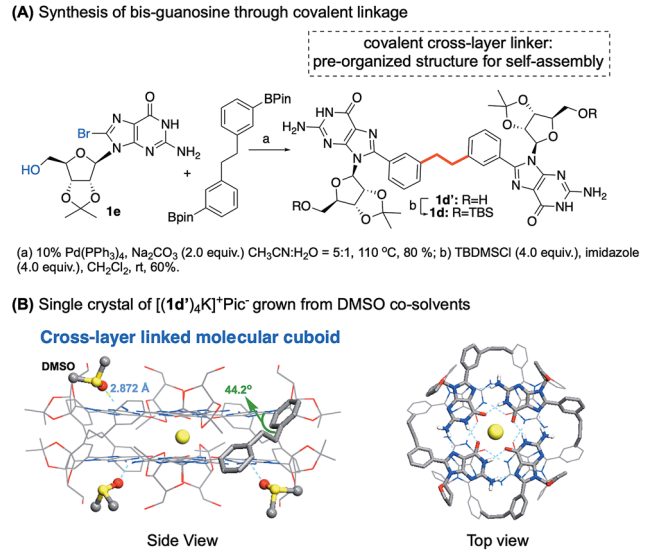

Fig. 5 (A) Synthesis of bis-guanosine derivatives. (B) Single crystal structure of $[(\mathbf{1d}')4K]^{+}\cdot(Pic^{-})$.§

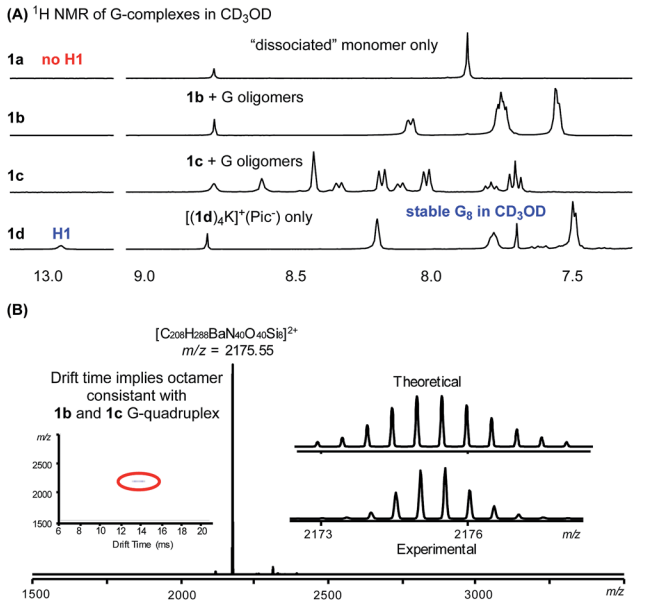

Fig. 6 (A) ^{1}H NMR spectra showing G-quadruplex stability in CD_3OD. (B) MS of $[(\mathbf{1d})_4Ba]^{2+}\cdot(Pic^{-})_2$ in MeOH.

Self-assembly of **1d** with K^{+} and Ba^{2+} cations in $CDCl_3$ gave a similar one-set of signals in the ^{1}H NMR spectra, consistent with the formation of a G_8-octamer. ESI-MS of complexes from **1d** and Ba^{2+} gave a doubly charged peak at $m/z = 2175.55$ as the dominant signal, indicating a mol. wt of 4351.1 for the supermolecule as $[(\mathbf{1d})_4Ba]^{2+}$. An attempt to obtain a single crystal of the **1d** complex failed initially, resulting in a rather thin, film-like solid formation. Fortunately, the single crystal structure was successfully obtained by switching the monomer to **1d**′ using DMSO as a co-solvent, confirming the cross-layer covalent linked structure as proposed (Fig. 5B). Notably, for complex $[(\mathbf{1d}')_4Ba]^{2+}\cdot(Pic^{-})_2$, the dihedral angle between 8-aryl and guanine is 40.7 degrees, similar to the dihedral angles in complex $[(\mathbf{1b})_8Ba]^{2+}\cdot(Pic^{-})_2$ (42.5 degrees). Overall, through G-monomer conformational analysis, a series of G_8-octamers was successfully prepared with functionalization at 8-phenyl (**1b**), a cross-layer H-bond linker (**1c**) and a covalent linker (**1d**).

G-quadruplex H-bond stability in MeOH

As discussed above, our intrinsic motivation in exploring these different G-quadruplexes was to develop H-bonded guanosine self-assembly that could survive in protic solvents (H-bond competitive). With all these different G_{16} and G_8 quadruplexes prepared, we dissolved them in CD_3OD to compare the ^{1}H NMR spectra. As shown in Fig. 6A, N(1)–H and N(2)–H protons did not appear in ^{1}H NMR spectra with CD_3OD as the solvent due to the H/D exchange. Thus, evaluation of the ^{1}H NMR spectra will mainly be focused on the non-exchangeable aromatic protons and ribose protons. Dissolving the G_{16}-hexadecamer $[(\mathbf{1a})_{16}K_4]^{4+}\cdot(Pic^{-})_4$ in CD_3OD gave only one set of signals, identical to the **1a** monomer in CD_3OD. The result suggested complete dissociation of the G_{16}-hexadecamer to **1a** monomer in MeOH. Interestingly, the G_8-octamer $[(\mathbf{1b})_8K]^{+}\cdot(Pic^{-})$ and $[(\mathbf{1c})_8K]^{+}\cdot(Pic^{-})$ in CD_3OD gave two sets of signals, indicating the existence of dissociated monomer and possible oligomers or a G-quadruplex in the solution phase. Although the exact structures of the guanosine species in these two cases are not determined at this moment, the fact that H-bonded guanosine complexes were formed with **1b** and **1c** clearly suggests the improved H-binding ability of these two monomers over **1a**. Surprisingly, when dissolving the G_8-octamer $[(\mathbf{1d})_4K]^{+}\cdot(Pic^{-})$ in CD_3OD, only one set of signals was observed. Notably, in this case, N(1)–H gave a broad signal at 12.95 ppm, clearly suggesting the formation of a G-quadruplex through a H-bond. NMR solvent signal suppression was applied for the G-quadruplex $[(\mathbf{1d})_4K]^{+}\cdot(Pic^{-})$ in CD_3OH. The peak at 12.9 ppm clearly showed up and was confirmed to be H1 of G in the G-quadruplex (see detailed NMR spectra in Fig. S7†). Thus, with monomer **1d**, a G-quadruplex remains intact in protic solvent CD_3OD. Impressively, this G-quadruplex did not dissociate even at elevated temperature in CD_3OD, with the N(1)H peak remaining at 60 °C (see Fig. S6† for VT NMR spectra). This observation indicated that there was a high kinetic barrier to break the **1d** G-quartet for H/D exchange, which highlighted the stability of $[(\mathbf{1d})_4K]^{+}\cdot(Pic^{-})$ in a H-bond competitive system. Injecting an MeOH solution of $[(\mathbf{1d})_4Ba]^{2+}\cdot(Pic^{-})_2$ complex into ESI-MS gave a dominant double charged peak with $m/z = 2175.55$, corresponding to $[(\mathbf{1d})_4Ba]^{2+}$ (Fig. 6B). It is noteworthy that TWIM-MS of this G-quadruplex in methanol solution was recorded as a single band ($m/z = 2175.55$) with drift time at 14.33 ms, which is in agreement with the size of the G_8-octamer (see detailed discussion in Table S1†). To the best of our knowledge, this is one of the few stable G-quadruplex systems from small molecule self-assembly to survive in a H-bond competitive environment.

Evaluating G-quadruplex stability

With the success in maintaining G-quadruplex stability in protic solvent MeOH, we sought to evaluate whether a similar

stability trend exists with polar aprotic solvents. DMSO is a strong polar solvent, which can disrupt the H-bond in G-quartets and cause the decomposition of G-quadruplexes. To evaluate how the incorporation of the phenyl group and cross-layer interaction impact on thermodynamic stability, G-quadruplexes were treated with $CDCl_3$/DMSO-d_6 solvent mixture. A summary of ^{1}H NMR spectra from these experiments is shown in Fig. 7.

As shown in the ^{1}H NMR spectra, G-quadruplexes from **1a**, **1b** and **1c** started to dissociate in mixed solvents containing 20% DMSO-d_6. Compared with the reported G_{16}-hexadecamer from **1a**,[46] the G_8-octamer formed by **1b** and **1c** showed comparable stability in 20% DMSO-d_6. Eventually, all three G-quadruplexes gave complete dissociation in 50% DMSO-d_6 solution with only one set of signals corresponding to the monomer. In contrast, $[(\mathbf{1d})_4K]^+\cdot(Pic^-)$ showed significantly improved stability, with only 2% complex dissociation in 50% DMSO-d_6. This result demonstrates the significantly enhanced stability of G-quadruplexes constructed by **1d**.

To quantify the thermodynamic stability of G-quadruplexes,[47] VT NMR experiments were carried out for pure complexes of $[(\mathbf{1a})_{16}K_4]^{4+}\cdot(Pic^-)_4$, $[(\mathbf{1b})_8K]^+\cdot(Pic^-)$, $[(\mathbf{1c})_8K]^+\cdot(Pic^-)$, and $[(\mathbf{1d})_4K]^+\cdot(Pic^-)$ in $CDCl_3$/DMSO-d_6 with a fraction of 20% DMSO-d_6. The values of complex dissociation enthalpy and entropy for each G-quadruplex were calculated from van't Hoff plots and are compared in Table S6 (see detailed discussion in the ESI†). For complex $[(\mathbf{1d})_4K]^+\cdot(Pic^-)$, no significant increase in monomer concentration was observed with the increase in temperature. This might be attributed to the high kinetic barrier for G-quadruplex $[(\mathbf{1d})_4K]^+\cdot(Pic^-)$ dissociation. To confirm this hypothesis, a NOESY experiment at 50 °C was performed for $[(\mathbf{1b})_8K]^+\cdot(Pic^-)$, $[(\mathbf{1c})_8K]^+\cdot(Pic^-)$ and $[(\mathbf{1d})_4K]^+\cdot(Pic^-)$ (Fig. S14–S16†). The results suggested that kinetic exchange between the complex and monomer for $[(\mathbf{1d})_4K]^+\cdot(Pic^-)$ was too slow to be recorded by NMR spectroscopy.

In addition to DMSO titration, the stability of G_8 and G_{16} complexes could also be evaluated using tandem-MS by increasing the operating voltage. The cation fragments of G-quadruplexes were separated and treated with increasing voltage. The operating voltage for G-quadruplex cation fragment decomposition are summarized in Table 2.

Table 2 Decomposition voltage

	$[(\mathbf{1a})_8Ba]^{2+}$	$[(\mathbf{1b})_8Ba]^{2+}$	$[(\mathbf{1c})_8Ba]^{2+}$	$[(\mathbf{1d})_4Ba]^{2+}$
Start[a]	30 V	40 V	50 V	70 V
End[a]	40 V	45 V	65 V	80 V

[a] Operating voltage (V).

It is noteworthy that $[(\mathbf{1a})_{16}Ba_2]^{4+}\cdot(Pic^-)_4$ only showed a doubly charged peak at m/z = 2123.31 corresponding to $[(\mathbf{1a})_8Ba]^{2+}$, indicating that the picrate bridge dissociated under the MS conditions. Further comparison of all the cation fragments of the G-quadruplexes revealed a clear stability trend as $[(\mathbf{1d})_4Ba]^{2+}$ > $[(\mathbf{1c})_8Ba]^{2+}$ > $[(\mathbf{1b})_8Ba]^{2+}$ > $[(\mathbf{1a})_8Ba]^{2+}$. Overall, the covalent linking strategy significantly helped to stabilize the G_8-octamer, both in H-bond competitive solvents and gas phase.

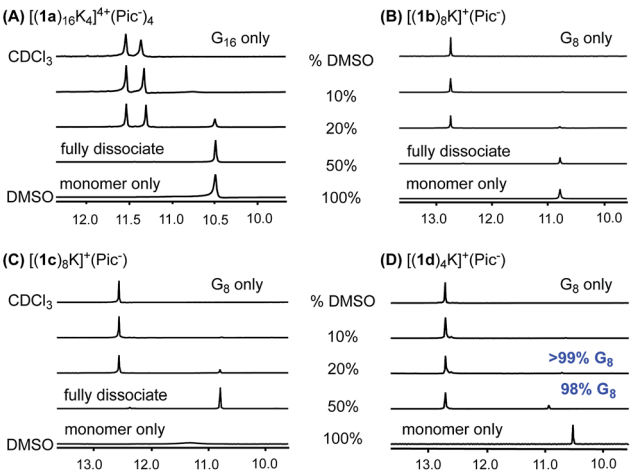

Fig. 7 DMSO-d_6 titration: ^{1}H NMR spectra of (A) $[(\mathbf{1a})_{16}K_4]^{4+}\cdot(Pic^-)_4$, (B) $[(\mathbf{1b})_8K]^+\cdot(Pic^-)$, (C) $[(\mathbf{1c})_8K]^+\cdot(Pic^-)$, (D) $[(\mathbf{1d})_4K]^+\cdot(Pic^-)$ in $CDCl_3$: DMSO-d_6 with DMSO-d_6 fractions of 10%, 20% and 50%.

Conclusions

In summary, with modification on both guanine (8-aryl) and ribose (sterically hindered 2′,3′ position), a stable G_8-octamer was formed with its structure characterized by single crystal X-ray diffraction for the first time. Through the analysis of cross-layer interactions, a covalently tethered 8-aryl guanosine dimer was designed and prepared for supramolecular assembly. The expected G_8-octamer was confirmed by X-ray, MS and NMR spectroscopy with significantly improved stability in MeOH and 1 : 1 DMSO/$CDCl_3$ mixture. To the best of our knowledge, this is the first example of discrete G-quadruplexes formed from small molecules with enhanced stability in a protic solvent (MeOH) and a polar aprotic solvent (DMSO). Meanwhile, formation of the stable G_8-octamer with a concise and well-defined bottom-to-bottom stacking mode provides a novel supramolecular platform. Incorporation of this new system into material and biological applications is expected and currently undergoing in our group.

Conflicts of interest

There are no conflicts to declare.

Acknowledgements

We are grateful to the NSF (CHE-1665122), the NIH (1R01GM120240-01), and NSFC (21629201) for financial support.

Notes and references

§ All the structures reported in this article have been deposited with the Cambridge Crystallographic Data Centre. The accession numbers for $[(\mathbf{1b})_8Ba]^{2+}\cdot(Pic^-)_2$; $[(\mathbf{1b})_8K]^+\cdot(PF_6^-)$; $[(\mathbf{1b})_8K]^+\cdot(Pic^-)$; $[(\mathbf{1b})_8Sr]^{2+}\cdot(Pic^-)_2$; $[(\mathbf{1b})_8Rb]^+\cdot(Pic^-)$; $[(\mathbf{1c})_8Ba]^{2+}\cdot(Pic^-)_2$; $[(\mathbf{1d}')_4K]^+\cdot(Pic^-)$ reported in this paper are:

1871565, 1871566, 1871567, 1871568, 1871569, 1871570, 1871754, correspondingly.

1 M. Fujita, *Structure and Bonding*, Springer, Berlin, 2000, pp. 177–201.
2 D. S. Lawrence, T. Jiang and M. Levett, *Chem. Rev.*, 1995, **95**, 2229–2260.
3 D. P. Craig and D. P. Mellor, *Structure and Bonding*, Springer, Berlin, 1976, pp. 1–48.
4 M. Fujita, *Chem. Soc. Rev.*, 1998, **27**, 417–425.
5 L. J. Prins, D. N. Reinhoudt and P. Timmerman, *Angew. Chem., Int. Ed.*, 2001, **40**, 2382–2426.
6 P. Y. W. Dankers and E. W. Meijer, *Bull. Chem. Soc. Jpn.*, 2007, **80**, 2047–2073.
7 H.-W. Jun, S. E. Paramonov and J. D. Hartgerink, *Soft Matter*, 2006, **2**, 177–181.
8 P. Xin, P. Zhu, P. Su, J.-L. Hou and Z.-T. Li, *J. Am. Chem. Soc.*, 2014, **136**, 13078–13081.
9 J. T. Davis, *Angew. Chem., Int. Ed.*, 2004, **43**, 668–698.
10 J. L. Sessler, C. M. Lawrence and J. Jayawickramarajah, *Chem. Soc. Rev.*, 2007, **36**, 314–325.
11 C. L. D. Gibb and B. C. Gibb, *J. Am. Chem. Soc.*, 2004, **126**, 11408–11409.
12 G. V. Oshovsky, D. N. Reinhoudt and W. Verboom, *Angew. Chem., Int. Ed.*, 2007, **46**, 2366–2393.
13 J. T. Davis and G. P. Spada, *Chem. Soc. Rev.*, 2007, **36**, 296–313.
14 G. P. Spada and G. Gottarelli, *Synlett*, 2004, **4**, 596–602.
15 E. Bouhoutsos-Brown, C. L. Marshall and T. J. Pinnavaia, *J. Am. Chem. Soc.*, 1982, **104**, 6576–6584.
16 J. P. N. V. Hud, *Quadruplex Nucleic Acids*, The Royal Society of Chemistry, Cambridge, 2006, pp. 100–130.
17 J. A. Walmsley, R. G. Barr, E. Bouhoutsos-Brown and T. J. Pinnavaia, *J. Phys. Chem.*, 1984, **88**, 2599–2605.
18 G. Biffi, M. Di Antonio, D. Tannahill and S. Balasubramanian, *Nat. Chem.*, 2013, **6**, 75.
19 J. N. Parkinson, *Quadruplex Nucleic Acids*, The Royal Society of Chemistry, Cambridge, 2006, pp. 1–30.
20 M. Zeraati, D. B. Langley, P. Schofield, A. L. Moye, R. Rouet, W. E. Hughes, T. M. Bryan, M. E. Dinger and D. Christ, *Nat. Chem.*, 2018, **10**, 631–637.
21 I. C. M. Kwan, Y.-M. She and G. Wu, *Can. J. Chem.*, 2011, **89**, 835–844.
22 M. a. D. C. Rivera-Sánchez, M. García-Arriaga, G. Hobley, A. V. Morales-de-Echegaray and J. M. Rivera, *ACS Omega*, 2017, **2**, 6619–6627.
23 M. d. C. Rivera-Sánchez, I. Andújar-de-Sanctis, M. García-Arriaga, V. Gubala, G. Hobley and J. M. Rivera, *J. Am. Chem. Soc.*, 2009, **131**, 10403–10405.
24 R. N. Das, Y. P. Kumar, O. M. Schütte, C. Steinem and J. Dash, *J. Am. Chem. Soc.*, 2015, **137**, 34–37.
25 S. L. Forman, J. C. Fettinger, S. Pieraccini, G. Gottarelli and J. T. Davis, *J. Am. Chem. Soc.*, 2000, **122**, 4060–4067.
26 M. S. Kaucher, W. A. Harrell and J. T. Davis, *J. Am. Chem. Soc.*, 2006, **128**, 38–39.
27 T. Bhattacharyya, P. Saha and J. Dash, *ACS Omega*, 2018, **3**, 2230–2241.
28 G. M. Peters and J. T. Davis, *Chem. Soc. Rev.*, 2016, **45**, 3188–3206.
29 G. M. Peters, L. P. Skala and J. T. Davis, *J. Am. Chem. Soc.*, 2016, **138**, 134–139.
30 M. García-Iglesias, T. Torres and D. González-Rodríguez, *Chem. Commun.*, 2016, **52**, 9446–9449.
31 D. González-Rodríguez, P. G. A. Janssen, R. Martín-Rapún, I. D. De Cat, S. De Feyter, A. P. H. J. Schenning and E. W. Meijer, *J. Am. Chem. Soc.*, 2010, **132**, 4710–4719.
32 H. Han and L. H. Hurley, *Trends Pharmacol. Sci.*, 2000, **21**, 136–142.
33 F. W. B. Van Leeuwen, W. Verboom, X. Shi, J. T. Davis and D. N. Reinhoudt, *J. Am. Chem. Soc.*, 2004, **126**, 16575–16581.
34 J. E. Betancourt, C. Subramani, J. L. Serrano-Velez, E. Rosa-Molinar, V. M. Rotello and J. M. Rivera, *Chem. Commun.*, 2010, **46**, 8537–8539.
35 S. Martic, G. Wu and S. Wang, *Inorg. Chem.*, 2008, **47**, 8315–8323.
36 J. M. Rivera, M. Martín-Hidalgo and J. C. Rivera-Ríos, *Org. Biomol. Chem.*, 2012, **10**, 7562–7565.
37 J. M. Rivera and D. Silva-Brenes, *Org. Lett.*, 2013, **15**, 2350–2353.
38 M. Martín-Hidalgo and J. M. Rivera, *Chem. Commun.*, 2011, **47**, 12485–12487.
39 K. B. Sutyak, P. Y. Zavalij, M. L. Robinson and J. T. Davis, *Chem. Commun.*, 2016, **52**, 11112–11115.
40 J. E. Betancourt, M. Martín-Hidalgo, V. Gubala and J. M. Rivera, *J. Am. Chem. Soc.*, 2009, **131**, 3186–3188.
41 D. González-Rodríguez, J. L. J. van Dongen, M. Lutz, A. L. Spek, A. P. H. J. Schenning and E. W. Meijer, *Nat. Chem.*, 2009, **1**, 151–155.
42 J. E. Betancourt and J. M. Rivera, *J. Am. Chem. Soc.*, 2009, **131**, 16666–16668.
43 J. E. Betancourt and J. M. Rivera, *Org. Lett.*, 2008, **10**, 2287–2290.
44 V. Gubala, J. E. Betancourt and J. M. Rivera, *Org. Lett.*, 2004, **6**, 4735–4738.
45 S. B. Zimmerman, *J. Mol. Biol.*, 1976, **106**, 663–672.
46 X. Shi, K. M. Mullaugh, J. C. Fettinger, Y. Jiang, S. A. Hofstadler and J. T. Davis, *J. Am. Chem. Soc.*, 2003, **125**, 10830–10841.
47 E. Fadaei, M. Martín-Arroyo, M. Tafazzoli and D. González-Rodríguez, *Org. Lett.*, 2017, **19**, 460–463.
48 M. García-Arriaga, G. Hobley and J. M. Rivera, *J. Am. Chem. Soc.*, 2008, **130**, 10492–10493.
49 A. L. Marlow, E. Mezzina, G. P. Spada, S. Masiero, J. T. Davis and G. Gottarelli, *J. Org. Chem.*, 1999, **64**, 5116–5123.
50 M. García-Arriaga, G. Hobley and J. M. Rivera, *J. Org. Chem.*, 2016, **81**, 6026–6035.
51 S. Lena, P. Neviani, S. Masiero, S. Pieraccini and G. P. Spada, *Angew. Chem., Int. Ed.*, 2010, **49**, 3657–3660.
52 S. Marti, X. Liu, S. Wang and G. Wu, *Chem.–Eur. J.*, 2008, **14**, 1196–1204.
53 X. Meng, T. Moriuchi, M. Kawahata, K. Yamaguchi and T. Hirao, *Chem. Commun.*, 2011, **47**, 4682–4864.
54 J. L. Sessler, M. Sathiosatham, K. Doerr, V. Lynch and K. A. Abboud, *Angew. Chem., Int. Ed.*, 2000, **39**, 1300–1303.

55 X. Shi, J. C. Fettinger and J. T. Davis, *Angew. Chem., Int. Ed.*, 2001, **40**, 2827–2831.
56 X. Shi, J. C. Fettinger and J. T. Davis, *J. Am. Chem. Soc.*, 2001, **123**, 6738–6739.
57 H. Wang, X. Qian, K. Wang, M. Su, W.-W. Haoyang, X. Jiang, R. Brzozowski, M. Wang, X. Gao, Y. Li, B. Xu, P. Eswara, X.-Q. Hao, W. Gong, J.-L. Hou, J. Cai and X. Li, *Nat. Commun.*, 2018, **9**, 1815.
58 J. G. Speight, *Lange's Handbook of Chemistry*, McGraw-Hill, New York, 16th edn, 2005, pp. 1–150.
59 R. Ida and G. Wu, *Chem. Commun.*, 2005, 4294–4296.